Effects of Layered Silicate Structure on the Mechanical Properties and Structures of Protein-Based Bionanocomposites

Peter R. Chang,[1] Yu Yang,[2] Jin Huang,[2] Wenbing Xia,[2] Liangdong Feng,[3] Jiangyu Wu[4]

[1]*Bioproducts and Bioprocesses National Science Program, Agriculture and Agri-Food Canada, Saskatoon, SK S7N 0X2, Canada*
[2]*College of Chemical Engineering, Department of Chemistry, College of Resource and Environmental Engineering, Wuhan University of Technology, Wuhan 430070, China*
[3]*Key Laboratory for Attapulgite Science and Applied Technology of Jiangsu Province, Department of Chemical Engineering, Huaiyin Institute of Technology, Huai'an 223003, China*
[4]*School of Material Science and Engineering, Wuhan Institute of Technology, Wuhan 430073, China*

Received 12 June 2008; accepted 12 January 2009
DOI 10.1002/app.30043
Published online 2 April 2009 in Wiley InterScience (www.interscience.wiley.com).

ABSTRACT: In this work, a nonconventional protein source of pea protein isolate (PPI) was filled with montmorillonite (MMT) and rectorite (REC) by solution intercalation respectively, and then the reinforced PPI-based nanocomposites were produced by hot press. The structure and interaction in the nanocomposites were investigated by FTIR, XRD, DSC, DMA, and pH and Zeta-potential tests whereas the reinforcing effect was verified by tensile test. Furthermore, the origin of enhancing mechanical performances and the effects of layered silicate structure were explored. Although the MMT with lower negative-charge surface and smaller apparent size of crude particles was easier to be exfoliated completely, the exfoliated REC nanoplatelets with more negative-charge could form stronger electrostatic interaction with positive-charge-rich domains of PPI molecules, and hence produced the highest strength in two series of nanocomposites. In this case, the newly formed hydrogen bonds and electrostatic interaction on the surface of silicate lamellas guaranteed the transferring of the stress to rigid layered silicates. The cooperative effect of newly formed physical interaction between layered silicates and PPI molecules as well as the spatial occupancy of intercalated agglomerates of layered silicates destroyed the original microphase structure of PPI matrix and cleaved the entanglements among PPI molecules. It was not in favor of enhancing the elongation and strength. © 2009 Wiley Periodicals, Inc. J Appl Polym Sci 113: 1247–1256, 2009

Key words: nanocomposite; layered silicate; protein; mechanical properties; structure–properties relationship

INTRODUCTION

Currently, biodegradable materials derived from renewable resources have been extensively developed and hence greatly improved the lives of human beings because of their environmental friendliness, i.e. avoiding the deposit of solid waste and debasing the environmental pollution as well as saving the limited fossil resources.[1] Protein is one of the few natural polymers that can be thermoplastic-processed under the plasticization of small molecules,[2,3] and shows a great potential for replacing the popular petroleum-based plastics. Although the plasticization can improve toughness and processability, it is pitiful that the strength inevitably decreases.[4] Moreover, the predominant role of the nano-filler in the nanocomposites for high mechanical properties brings about the development of "green" protein-based bionanocomposites.[5] The exfoliated lamella of layered silicates strongly adhered onto the soy protein matrix by electrostatic affiliating as well as hydrogen bonding to produce reinforced materials.[6,7] The nano-clusters of aggregated spherical SiO_2 nanoparticles[8] and flexible carbon nanotubes[9] played a role on reinforcing and toughening soy protein plastics simultaneously. Meanwhile, the biodegradable polysaccharide nanoparticles, such as rod-like cellulose[10] and chitin[11] whiskers, and platelet-like starch nanocrystal,[12] were used to reinforce

Correspondence to: P. R. Chang (changp@agr.gc.ca) or J. Huang (huangjin@iccas.ac.cn).

Contract grant sponsor: Agricultural Bioproducts Innovation Program (ABIP) of Canada [via the Pulse Research Network (PURENet)].
Contract grant sponsor: National Natural Science Foundation of China; contract grant number: 50843031.
Contract grant sponsor: Natural Science Foundation of Jiangsu Province of China; contract grant number: BK2008196.
Contract grant sponsor: Youth Chenguang Program of Science and Technology in Wuhan; contract grant number: 200850731383.

soy protein as well as enhancing water resistance. In addition, the hydroxylpropyl lignin can spontaneously assemble as oblate supramolecular nanoaggregates in soy protein matrix to enhance the strength of materials.[13,14]

A considerable attention has been concentrated on exploring the mechanisms of intercalation and exfoliation in academic opinions and developing high-performance and low-cost materials for meeting practical applications, owing to the great improvement of performances over pristine polymer,[15] such as reinforcing function,[16] reducing gas permeability,[17] enhancing thermal stability[18] and self-extinguishing fire-retardance,[19] and other interesting properties. Montmorillonite (MMT) is currently the most popular in the family of layered silicates,[20] and its nylon-based nanocomposite was taken as a representative example for the reinforcing effect. It played a key role in the expansion of gallery distance and even exfoliation of lamellae that the metal cations, attached to the interlayer surface with net negative charge of parallel stacking sandwiched lamella, can ion-exchange by the polar group of nylon.[21] The ability of ion exchange for various layered silicates is dominated by the structure of interlayer surface, especially for the cationic character. In contrast with 2 : 1 layered structure of MMT[22] (two fused silicate tetrahedral sheets sandwiching an edge-shared octahedral sheet of either aluminum or magnesium hydroxide), rectorite (REC) is defined as a layer structure arranged regularly with the alternate pairs of dioctahedral micalike layer (nonexpansible) and dioctahedral smectitelike layer (expansible) in a 1 : 1 ratio.[23] In addition, compared with the popular MMT of about 1 μm in length as well as in width, the original REC single sheet, i.e. the sum of the thickness of the smectite layer and the thickness of the mica layer, is about 40 μm in length and 5 μm in width. As a result, the separable layer thickness and layer aspect ratio (width vs. thickness) of REC are larger than those of regular MMT. Especially, the interlayer spacing of REC can reach about 2.4 nm as twice as the MMT interlayer spacing of about 1.2 nm. As well known, the narrow gallery of layered silicates is a key factor to inhibit the insertion of polymer chains into interlayer owing to the higher gyration radius of typical polymers. Consequently, the REC can be easier to be intercalated by the polymer chains.

In view of the success of reinforcing soy protein plastics by incorporating layered silicates mentioned above,[6,16] another protein source of pea protein isolate (PPI) was filled with MMT and REC by solution intercalation respectively, and then the reinforced PPI-based nanocomposites were produced by hot press. In this case, the facile exfoliation of MMT and REC as well as the resultant high mechanical performances was expected. Based on the structural characters of MMT and REC, the exfoliated extent of layered silicates and the interfacial interaction at the surface of lamellae, which determined mechanical performances, were obviously different. Consequently, we investigated the structure and properties of PPI/MMT- and PPI/REC-based nanocomposites, and hence distinguished the effects of the layered silicate structure.

EXPERIMENTAL

Material

PPI (commercial name as Propulse^{TM}) was a gift from Nutri-Pea Ltd. (Portage La Prairie, MB, Canada), and contained 6% moisture, <4% ash, <3% lipids, <12% carbohydrates, and 82% protein, according to the manufacturer's analytical results. REC and Na^+ –MMT, (NANNOLIN DK0) were supplied by Hubei Celebrities Rectorite Technology Co. (Hubei, China) and by Fenghong Clay Chemical Corporation in China, respectively. The cation exchange capacity of REC was 40 meq/100 g with a particle dimension of $\sim$ 40 mm in length and 5 μm in width while the cation exchange capacity of MMT was 110 meq/100 g with a particle dimension of 25 $\times$ 1000 nm in dry state. Glycerol purchased from the Shanghai Chemical Co. (Shanghai, China) was of analytical grade.

Preparation of PPI-based nanocomposite powders

PPI (10 g) was dissolved in 150 mL distilled water at room temperature with mechanical stirring (300 rpm) to obtain an emulsion. At the same time, a desired amount of layered silicate (REC or MMT) was also ultrasonically dispersed in 50 mL distilled water followed by mechanical stirring (300 rpm) for 30 min. Subsequently, the suspension of layered silicate was added to PPI emulsion with strong dispersion (800 rpm) at ambient temperature for 12 h to produce a homogeneous blend. The resultant viscous solution (dark-gray for the REC/PPI blends and light-yellow for the MMT/PPI blends) was freeze-dried for 48 h to obtain the nanocomposites (gray REC/PPI powder or yellow MMT/PPI powder), which preserved the original complex state in solution. According to the REC content in solid powders of 2, 4, 8, 12, 16, 20, and 24 wt %, the gray nanocomposite powders were coded as RP-2-P, RP-4-P, RP-8-P, RP-12-P, RP-16-P, RP-20-P, and RP-24-P, respectively. Meanwhile, the yellow nanocomposite powders containing 2, 4, 8, 12, 16, 20, and 24 wt % MMT were coded as MP-2-P, MP-4-P, MP-8-P, MP-12-P, MP-16-P, MP-20-P, and MP-24-P, respectively.

Compression-molding of PPI-based nanocomposite sheets

The RP-P and MP-P powders were melt-mixed with the plasticizer of glycerol in an intensive mixer (Thermo Haake Rheomix) for 10 min at a temperature of 140°C, and the weight ratio of every solid powder and glycerol was controlled as 70 : 30 all the time. Subsequently, 5 g of glycerol-plasticized powders were compression-molded with a 769YP-24B hot-press (Keqi High Technology Co., Tianjin, China) as sheets at 140°C under the pressure of 20 MPa for 3 min, and then air-cooled to 50°C for half an hour before releasing pressure for demolding. The dimension of the resultant sheets with the thickness of *ca*. 0.5 mm was about 70 mm × 70 mm. According to the codes of the original powders, the molded sheets were coded as RP-2-S, RP-4-S, RP-8-S, RP-12-S, RP-16-S, RP-20-S, RP-24-S, MP-2-S, MP-4-S, MP-8-S, MP-12-S, MP-16-S, MP-20-S, and MP-24-S, respectively. The molded sheets containing REC showed a gray color whereas other molded sheets containing MMT showed a yellow color and were more transparent than those REC-based sheets. In addition, the pure glycerol-plasticized PPI powder was also compression-molded as a sheet by the same process mentioned above, and coded as PPI-S.

Characterization

The pH-values were measured using a pH analyzer (Model PH-3D PH Meter, Shanghai, China) whereas ζ-potential analysis was carried out on a Zeta potential/particle sizer Nicomp 380ZLC apparatus (Santa Barbara, USA). The requisite PPI-based suspensions containing various REC and MMT contents for the pH-value and ζ-potential analysis were prepared through a process as the preparation of the RP-P and MP-P nanocomposite powders.

Fourier transform infrared spectra (FTIR) were recorded on a 5700 spectrometer (Nicolet, USA) in a range of 4000–400 cm^{-1} using a KBr-pellet method. X-ray diffraction (XRD) measurements were performed on a D8 Advance diffractometer (Bruker) equipped Kα radiation source (β = 0.154 nm). The diffraction data were collected in the range of 2θ = 1–10° using a fixed time mode with a step interval of 0.02°.

DSC analysis was carried out on a DSC-204 instrument (Netzsch, Germany) under nitrogen atmosphere at a heating or cooling rate of 20°C min^{-1}. The sheets were scanned in the range of −150 to 100°C after a pretreatment (heating from 20 to 100°C and then cooling down to −150°C) of eliminating the thermal history. DMA measurement was carried out on a DMA-242C dynamic mechanical analyzer (Netzsch, Germany) at a frequency of 1 Hz in the range from −150°C to 100°C with a heating rate of 3°C min^{-1}. A dual cantilever device was used while the specimen size was 40 × 10 × *ca*. 0.5 mm^3.

The tensile strength (σ_b), elongation at break (ε_b), and Young's modulus (E) of the sheets were measured on a universal testing machine (CMT6503, Shenzhen SANS Test Machine Co., Shenzhen, China) with a tensile rate of 5 mm min^{-1} according to GB13022-91. The tested sample's distance between the testing marks was 40 mm. An average value of five replicates of each sample was taken.

RESULTS AND DISCUSSION

Exfoliation and intercalation of layered silicates in PPI matrix

By virtue of higher motion ability in solution, polymer chains can penetrate into the gallery of layered silicate (REC and MMT). Subsequently, the interlayer distances of the freeze-dried RP-P and MP-P powders, which preserved the original states after solution intercalation, were investigated by XRD patterns (Fig. 1). The pristine REC in Figure 1(A) had two dominant peaks located at 3.52° (d_{001} = 2.43 nm) and 7.10° (d_{002} = 1.10nm)[24] whereas the d-spacing of MMT was verified by Figure 1(B) as *ca*. 1.26–1.44 nm. At the same time, the neat PPI powder had no diffraction in a range of 1–10°. As shown in Figure 1(A,B), the exfoliation and intercalation of REC and MMT obviously depended upon the loading-level of layered silicates. When the REC content was lower than 4 wt %, the REC was almost completely exfoliated in the RP-P powders. Furthermore, the loading-level of complete exfoliation of MMT could reach 8 wt %. It indicated that the MMT was easier to exfoliate. With a continuous increase of the loading-level of layered silicates, the intercalated components gradually increased whereas the interlayer distances became narrower, together with the inevitable increase of exfoliated nanoplatelets.[25] As regard to the RP-P powders with higher loading-level of REC, the diffraction peaks marked as I and II shifted to wide angle together with the increase of diffraction intensities. At the same time, the values of peak III and onset IV assigned to the diffraction of intercalated MMT shifted to wide angle as well with an increase of MMT content in nanocomposite powders. It suggested that excess loading-level inhibited the penetration of the PPI molecules into the gallery of interlayer to expand the interlayer distances.[6,16]

As shown in Figure 2[(A)-III,(B)-III], there existed two groups of vibrations associated with the Si—O groups in layered silicates, such as in-plane Si—O stretching (1122, 1051 and 1023 cm^{-1}) and out-of-plane Si—O stretching (1086 cm^{-1}) for the RP-P as

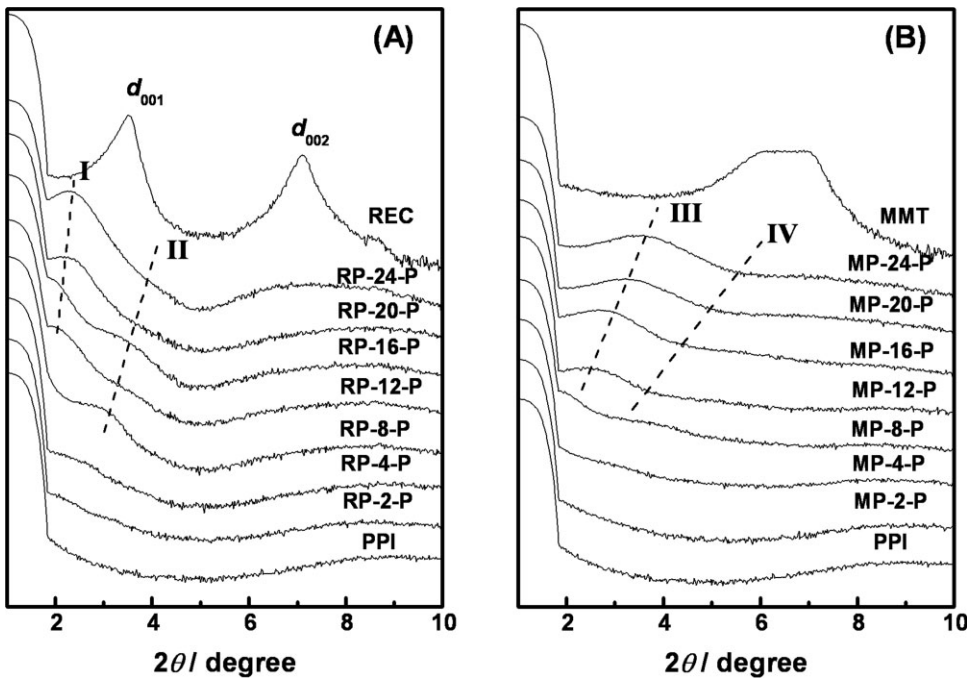

Figure 1 XRD patterns of the nanocomposite powders based on various loading-level of layered silicates (REC for A and MMT for B) and PPI as well as the powders of neat PPI, REC and MMT.

well as in-plane Si—O stretching (1120, 1038 and 1010 cm^{-1}) and out-of-plane Si—O stretching (1086 cm^{-1}) for the MP-P.[26] It is noted that the out-of-plane Si—O stretching located at 1086 cm^{-1} is related to the orientation of the lamella of layered silicates. Especially, the disordering of the lamellas should result in the increase of such band intensity.[26,27] As a result, the increasing intensity at 1086 cm^{-1} for two series of nanocomposite powders, compared with the neat REC and MMT powders, suggested that there were many lamellas of layered silicates to be exfoliated and disorderly dispersed into PPI matrix. It not only verified the XRD results, but further proved that there were still exfoliated lamellas in PPI matrix in spite that the XRD patterns showed predominant intercalation character.

Hydrogen bonding between layered silicates and PPI

The exfoliation and intercalation of layered silicates strongly depended upon the formation of hydrogen bonds and electrostatic affiliation between the PPI molecules and the interlayer surface of layered silicates. As well-known, the Si—O—Si and —OH groups onto the layered silicates of REC and MMT could be hydrogen bonded with the polar groups in the PPI molecules, such as —NH, —C=O and so on, respectively.[28,29] Figure 2(A)-I showed the O—H stretching (the peaks located at 3645 and 3429 cm^{-1}) onto REC[30] and a brand (the peak located at 3441 cm^{-1}) of PPI including the N—H and O—H stretching. However, in the RP nanocomposite powders, the absorption located at low wavenumber of 3285 cm^{-1} could be clearly identified. It indicated that the new hydrogen bonds, associated with —NH in PPI as well as —OH in REC, formed. With an increase of REC content, the absorption assigned to newly hydrogen bonding decreased. Meanwhile, the peak located at 3645 cm^{-1} occurred for RP-12-P, and the increase of intensity was in good agreement with the increase of REC content. In view of the increase of intercalated REC component proved by XRD results with an increase of REC content, it suggested that the narrower gallery in intercalated structure inhibited the forming of new hydrogen bonds. In spite that there were some differences on the location of absorption in Figure 2(B)-I, the same conclusion can be drawn for the MP-P nanocomposites.

The formation of new hydrogen bonds can be also verified by the shift to low frequency and increasing intensity of amide II (N—H bending and C—N stretching modes) in Figure 2(A)-II,(B)-II functioned as the loading-level of layered silicates. Meanwhile, the weakening of the free —C=O peaks located at 1731 cm^{-1} for the RP-P and at 1727 cm^{-1} for the MP-P indicated that more —C=O groups in PPI molecules participated into the forming of hydrogen bonds. At the same time, in view of the obvious change of the Si—O stretching in Figure 2(A)-III,(B)-III, it is believed that the sites of newly hydrogen bonding included the oxygen atoms on the silicate layer surface and the hydrogen atoms in —NH of the peptide bonds.[31]

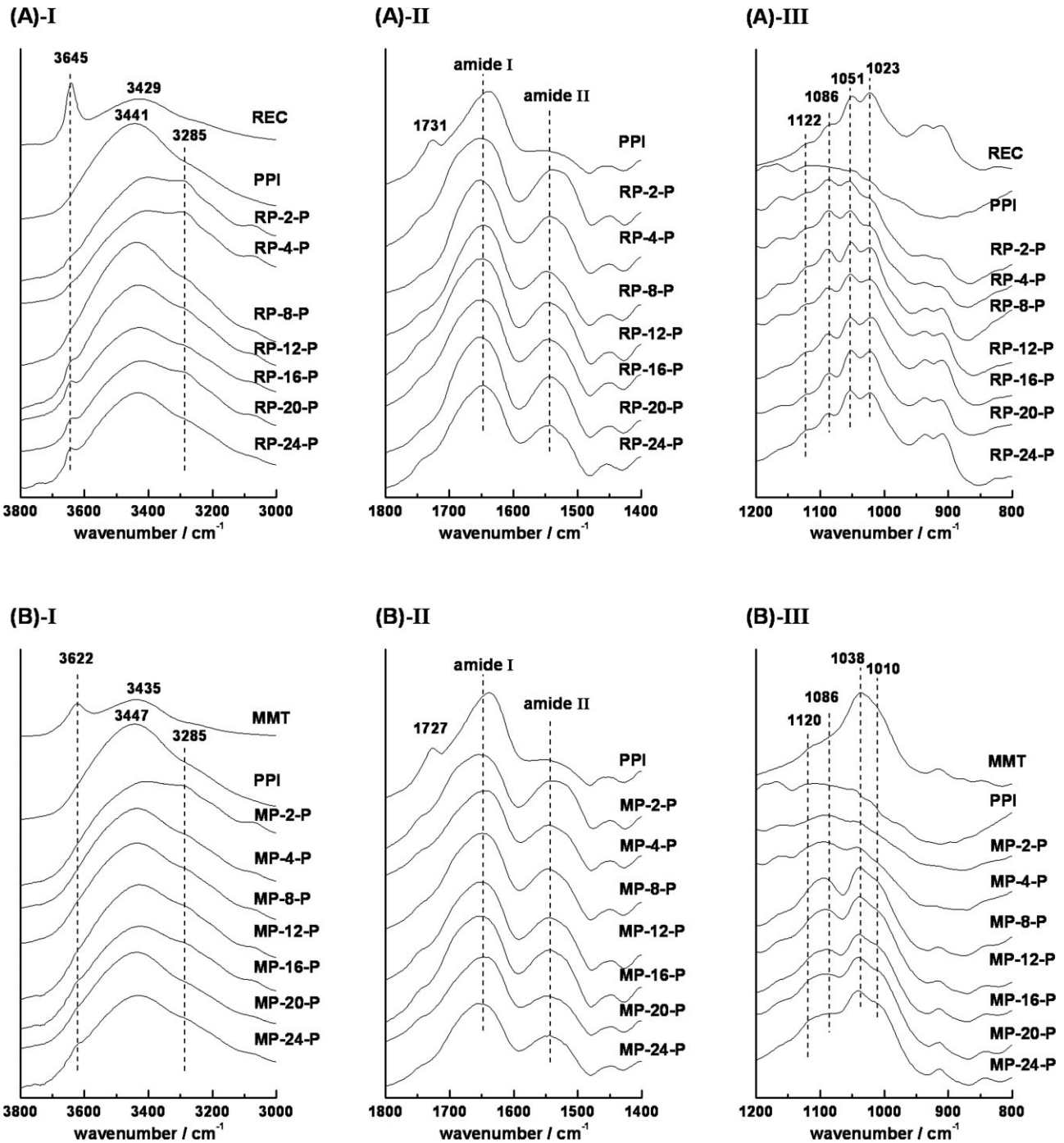

Figure 2 Three FTIR regions of 3800–3000 cm^{-1} (I), 1800–1400 cm^{-1} (II), and 1200–800 cm^{-1} (III) for the nanocomposite powders based on various loading-level of layered silicates (REC for A and MMT for B) and PPI as well as the powders of neat PPI, REC, and MMT.

Electrostatic interaction between layered silicates and PPI

The electrostatic affiliation between the layered silicates (REC and MMT) and PPI was investigated by the tests of pH and Zeta potential. Figure 3 shows the pH values of nanocomposite suspensions functioned as the loading-level of layered silicates (REC and MMT) as well as the pure REC and MMT suspension with the same concentration in the nanocomposite suspension and the neat PPI emulsion. The REC suspension with the lowest concentration had a pH of 6.09, and slightly decreased down to 5.84 with an increase of the REC concentration. Meanwhile, the pH of the MMT suspension with the lowest concentration was 7.84, and increased up to 8.89 as the MMT concentration increased. In contrast with the pH 7.35 of PPI, the pH values of the RP-P suspensions increased from 6.80 to 7.73 in the

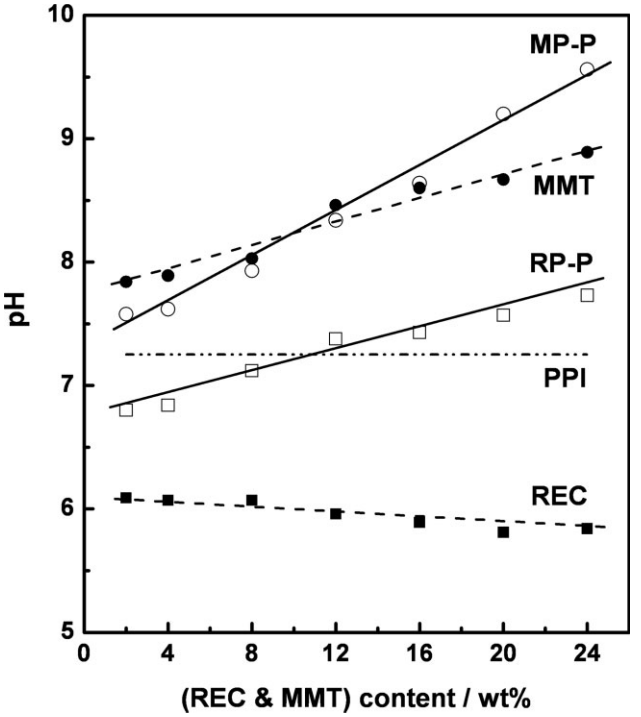

Figure 3 Dependence of pH values on the loading-level of layered silicates (REC and MMT) for the PPI/layered silicates suspensions and the suspensions of layered silicates (REC and MMT) with the same concentration as well as the pH values of the PPI emulsion.

loading-level range of 2–24 wt % whereas the pH values of the MP-P suspensions increased from 7.58 to 9.56. In contrast with almost no change of pH for the blends of MMT and soy protein isolate,[6] the MP-P system showed an obvious increase in the pH values. It indicated that the addition of MMT changed the electrostatic surface potential of PPI molecules. When the MMT was almost exfoliated completely (proved by the XRD results), the pH values of nanocomposite suspensions were lower than those of the corresponding MMT suspensions. However, when the loading-level of MMT was higher than 12 wt %, the inhibition to the exfoliation and intercalation of MMT resulted in higher pH values in contrast with those of the corresponding MMT suspensions. As regard to the RP-P system, the pH values of the nanocomposite suspensions increased with an increase of the REC content as well. When the REC content was higher than 12 wt %, the pH values of nanocomposite suspensions with obvious intercalation character were higher than that of neat PPI suspension. It also suggested that the electrostatic surface potential of PPI molecules was changed after introducing REC. Consequently, the changes of electrostatic surface potential might result from the electrostatic interaction between PPI molecules and layered silicates and be dependent upon the exfoliation and intercalation states of layered silicates.

Figure 4 shows the effects of the loading-level of REC and MMT on the Zeta-potential (ζ) of the nanocomposite suspensions, which was used to further disclose the electrostatic interaction in the nanocomposites. The ζ values of PPI, REC, and MMT showed net-negative character whereas that of PPI was intervenient between REC and MMT. The combination of net-negative PPI and net-negative layered silicates was attributed to the existence of positive-charge-rich domains in PPI molecules, as proved by previous report.[6] When the REC with the lowest ζ value was added, the ζ value of the RP-P nanocomposites firstly decreased until the loading-level of 8 wt %, and then increased. In this case, all the nanocomposites had the ζ values intervenient between REC and neat PPI. It indicated that the surface of REC in the nanocomposites was covered with PPI molecules, and hence produced the electrostatic interaction on the surface of the REC lamellas.[32,33] At the same time, when the MMT with higher ζ value than PPI was added, the ζ value of the MP-P nanocomposites firstly increased until the loading-level of 8 wt %, and then decreased. When the MMT content was higher than 16 wt %, the ζ values were even lower than that of neat PPI. It suggested that the structure of positive-charge-rich and negative-charge-rich domains in PPI molecules was destroyed to some extent in the process of forming interaction between PPI molecules and layered silicates.

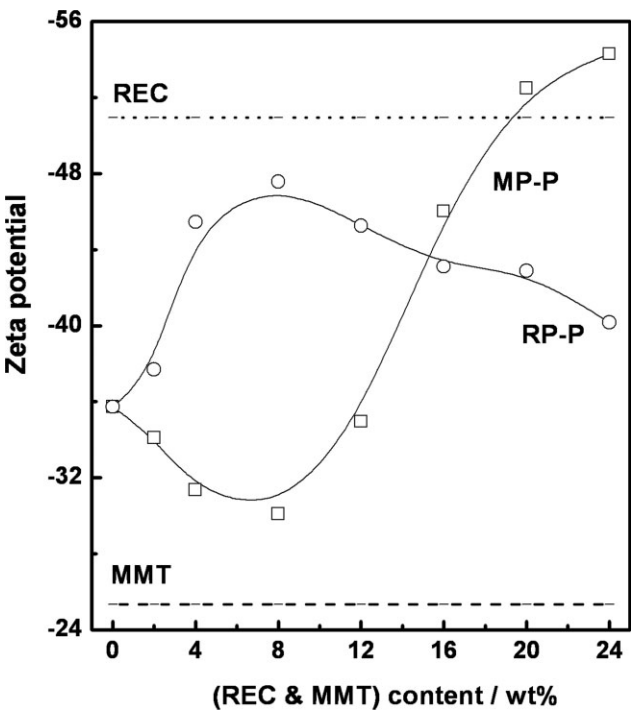

Figure 4 Dependence of Zeta-potential (ζ) on the loading-level of layered silicates (REC and MMT) for the PPI/layered silicates suspensions as well as the ζ-potential of neat PPI, REC and MMT.

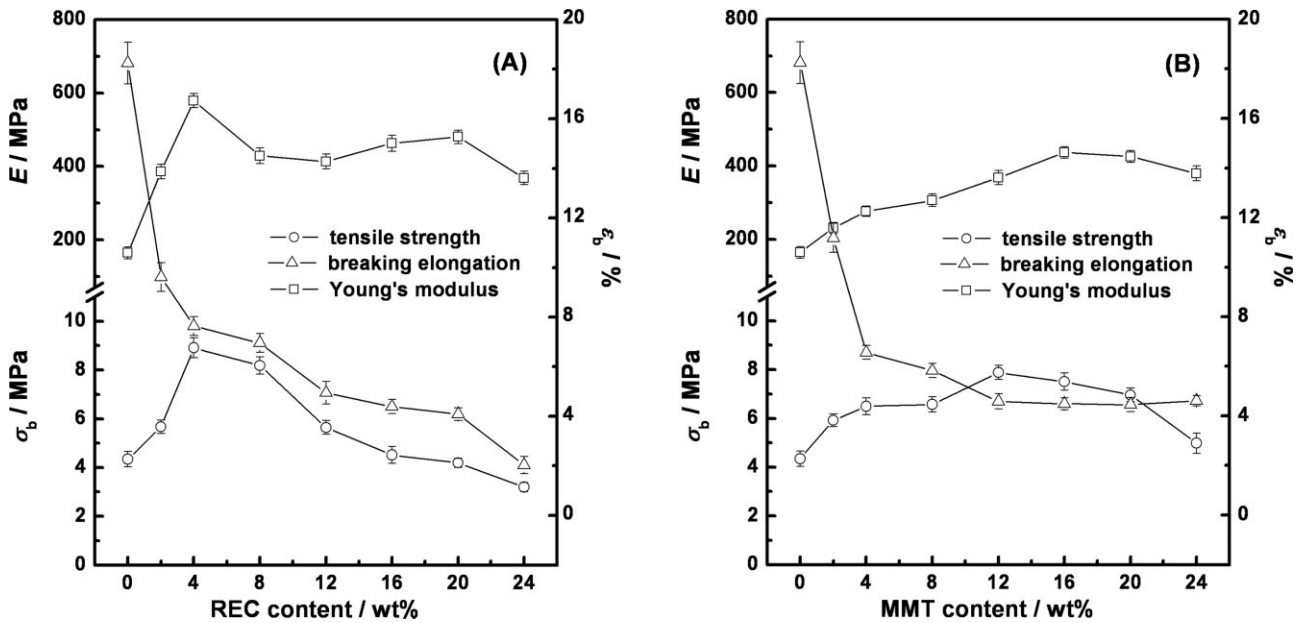

Figure 5 Effects of the loading-level of layered silicates (REC for A and MMT for B) on tensile strength (σ_b), elongation at break (ε_b) and Young's modulus (E) for the molded nanocomposite sheets based on PPI and layered silicates.

Mechanical properties of PPI-based nanocomposite sheets

With an assistance of glycerol as plasticizer, the RP-P and MP-P nanocomposite powders were compression-molded as sheets. Figure 5 shows the mechanical properties of the molded RP-S and MP-S sheets containing various loading-levels of layered silicates (REC or MMT), including tensile strength (σ_b), elongation at break (ε_b) and Young's modulus (E). The addition of REC and MMT could obviously enhance the strength and modulus of the PPI sheet. It offsets the decrease of strength due to the plasticization of glycerol. For the RP-S nanocomposites, the strength firstly increased, and reached the maximum value as 2-fold over neat PPI-S when the loading-level of REC was 4 wt %. Thereafter, with a continuous increase of REC content, the strength gradually decreased and was even lower than neat PPI-S when the REC content was higher than 16 wt %, attributing to decreasing effective surface of the unexfoliated REC agglomerates for forming hydrogen bonds and electrostatic interaction. The dependence of Young's modulus upon the REC content was similar to that of strength except that the nanocomposites containing the REC of higher than 16 wt % had increasing Young's modulus followed by a decrease. The rigidity of the REC agglomerates contributed to the increase of Young's modulus. However, when the loading-level was too high (i.e. higher than 16 wt %), the severer breakage of PPI matrix resulted in the decrease of Young's modulus. Meanwhile, with an increase of REC content, the elongation continually decreased owing to the cleavage of entanglements among PPI molecules.

For the MP-P nnaocomposites, with an increase of MMT content, the strength firstly increased and reached the maximum value as 1.8-fold over neat PPI-S when the loading-level of MMT was 12 wt %, followed by a slight decrease. All the MP-S sheets showed higher strength than PPI-S due to smaller size of the unexfoliated MMT agglomerates. It decreased the breakage of original structure in PPI matrix. Meanwhile, the dependence of Young's modulus upon the MMT content was similar to that of strength except that the loading-level of 16 wt % corresponded to the highest Young's modulus. Different from the predominant function of the exfoliated MMT nanoplatelets for enhancing strength, the enhancement of Young's modulus was attributed to the synergic effect of the exfoliated nanoplatelets and intercalated agglomerates. Furthermore, with an increase of MMT content, the cleavage of entanglements among PPI molecules resulted in the gradual decrease of elongation as well.

Thermal properties of PPI-based nanocomposite sheets

DSC and DMA were used to further realize the interaction between PPI and layered silicates (REC and MMT) together with the structural changes in the nanocomposite sheets. Figure 6 depicts the DSC thermograms of the RP-S and MP-S sheets, and data of glass transition temperature at midpoint ($T_{g,mid}$) and heat-capacity increment (ΔC_p) are summarized in Table I. Except the RP-4-S sheet, the other RP-S sheets with higher loading-levels had lower $T_{g,mid}$s

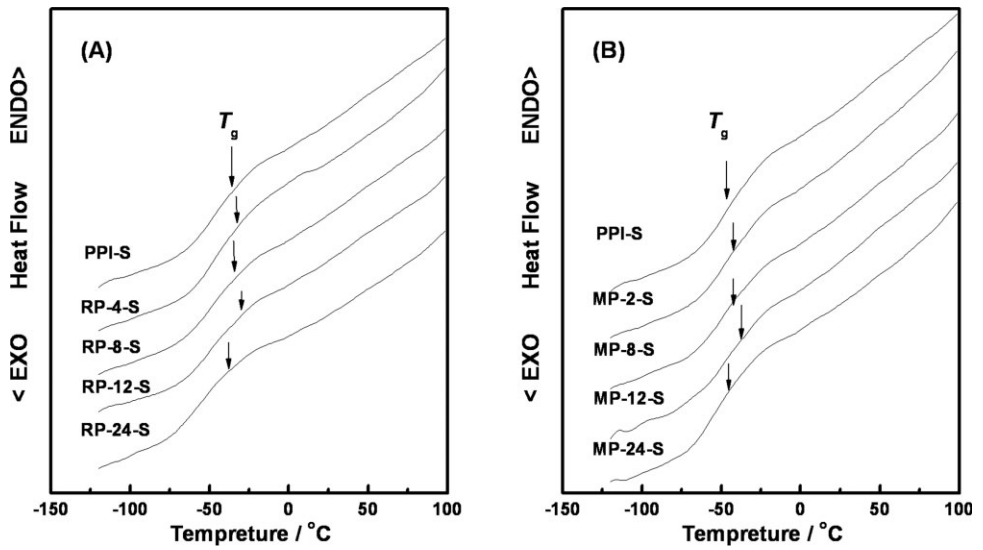

Figure 6 DSC thermograms of the nanocomposite sheets based on various loading-levels of layered silicates (REC for A and MMT for B) and PPI as well as the PPI-S sheet as reference.

than PPI-S. In the nanocomposites, the motion of PPI segments might be restricted by the exfoliated lamellas of layered silicates and the agglomerates of the intercalated layered silicates, depending upon hydrogen bonding and electrostatic affiliation on the surface of silicate lamella. On the other hand, the nanoplatelets and agglomerates of layered silicates could destroy the original structure of PPI matrix, and hence provided higher freedom of motion for the PPI segments. In this case, higher $T_{g,mid}$ of RP-4-S was attributed to the strong interaction on the surface of exfoliated lamellas and less breakage of PPI matrix. However, with an increase of REC content, the REC agglomerates with lower effective surface occurred. At this time, lower $T_{g,mid}$s indicated severe breakage of original structure in PPI matrix, and especially for the cleavage of entanglements. With a continuous increase of REC content, the $T_{g,mid}$s gradually shifted to low temperature. It suggested that the extent of breaking PPI matrix increased. As regard to the MP-S sheets, the same origin resulted in the changes of $T_{g,mid}$s similar to those for the RP-S sheets.

However, the α-relaxation temperatures from log E–T curves ($T_{\alpha,onset}$s) and from tan δ–T curves ($T_{\alpha,max}$s) in Figure 7 of all the nanocomposite sheets, measured by DMA, were lower than those of PPI-S. Table II summarizes the $T_{\alpha,onset}$s and log E_{onset}s as well as $T_{\alpha,max}$s and $H_{loss\text{-}peak}$s for the tested nanocomposite sheets and PPI-S. In contrast with the glass transition on domain-scale measured by DSC, DMA can reflect the freedom of segments at the molecular-level by observing α-relaxation. As a result, decreasing $T_{\alpha,onset}$s and $T_{\alpha,max}$s of all the nanocomposite sheets indicated that the original entanglements and interactions among PPI molecules might be partly destroyed whereas newly formed interactions between layered silicates and PPI molecules were weaker than the original state in PPI matrix. Meanwhile, the decreasing log E_{onset}s also verified the cleavage of the original structure in PPI matrix in spite of the occurrence of newly forming interaction between layered silicates and PPI molecules. With an increase of the layered silicate content, the log E_{onset}s gradually increased. It suggested that the aggregation of the layered silicates decreased the effective interaction with the PPI molecules and the cleavage of the original structure in the PPI matrix. When the content of layered silicates increased up to

TABLE I
DSC Data of the Nanocomposite Sheets of RP-S and MP-S Containing Various Loading-Levels of Layered Silicates as Well as Neat PPI-S Sheet

Sample code	$T_{g,mid}$/°C	ΔC_p/J g^{-1} K^{-1}	Sample code	$T_{g,mid}$/°C	ΔC_p/J g^{-1} K^{-1}
RP-4-S	−42.2	0.471	MP-2-S	−44.6	0.410
RP-8-S	−46.6	0.392	MP-8-S	−46.4	0.380
RP-12-S	−46.8	0.399	MP-12-S	−45.8	0.409
RP-24-S	−52.8	0.406	MP-24-S	−50.2	0.428
PPI-S	−45.4	0.421			

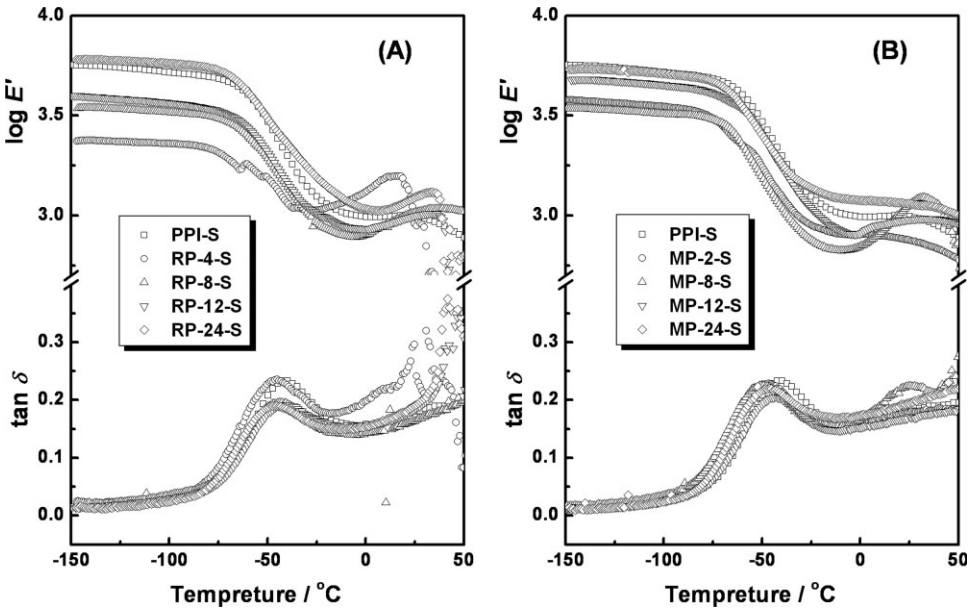

Figure 7 Logarithm of storage modulus (log E') and tangent of loss angle (tan δ) functioned as temperature for the nanocomposite sheets based on various loading-levels of layered silicates (REC for A and MMT for B) and PPI as well as the PPI-S sheet as reference.

24 wt %, the log E_{onset}s were equal to that of PPI-S in spite of the inevitable breakage of original structure in the PPI matrix. It verified the reinforcing role of the layered silicates as filler. As a result, in view of the enhancement of strength and Young's modulus after adding layered silicates, newly formed hydrogen bonds and electrostatic interaction on the surface of silicate lamellas guaranteed the transferring of the stress to rigid layered silicates at least.

Effects of layered silicate structure on the structure and mechanical properties

As mentioned in the Introduction and Experimental sections, the REC and MMT showed the obvious differences in apparent size, layer stacking, interlayer distance, and surface composition. It affected the extents of exfoliation and intercalation as well as physical interaction on the surface of silicate lamellas. In our study, the ζ value of REC was lower than that of PPI, but MMT had higher ζ value in contrast to PPI. As a result, the REC with more negative charge on the surface of lamellas could produce stronger electrostatic interaction with the positive-charge-rich domain of PPI molecules. Meanwhile, the nanocomposite sheet containing REC with an optimal loading-level of 4 wt % had higher strength in contrast to the MP-12-S sheet with the highest strength in the MP-S sheets. However, the wider distance of interlayer in REC could not increase the efficiency of exfoliation, namely the loading-level of complete exfoliation for REC (4 wt %) was lower than 8 wt % for MMT. In view that the PPI, REC, and MMT were net-negative, the electrostatic repulsion was inevitable. Consequently, it can be deduced that the key driving force of exfoliation, i.e. the electrostatic interaction between REC and the positive-charge-rich domains of PPI molecules, was inhibited. In addition, a greater size of crude REC particles, in contrast with MMT, might result in more residue of intercalated

TABLE II
DMA Data of the Nanocomposite Sheets of RP-S and MP-S Containing Various Loading-Levels of Layered Silicates as Well as Neat PPI-S Sheet

Sample code	log E–T curve		tan δ–T curve		Sample code	log E–T curve		tan δ–T curve	
	$T_{\alpha,onset}$/°C	log E_{onset}/MPa	$T_{\alpha,max}$/°C	$H_{loss\text{-}peak}$		$T_{\alpha,onset}$/°C	log E_{onset}/MPa	$T_{\alpha,max}$/°C	$H_{loss\text{-}peak}$
RP-4-S	−84.6	3.35	−45.1	0.236	MP-2-S	−77.5	3.52	−46.8	0.229
RP-8-S	−79.6	3.50	−43.6	0.196	MP-8-S	−79.0	3.50	−49.4	0.225
RP-12-S	−74.1	3.53	−42.9	0.191	MP-12-S	−76.1	3.62	−43.1	0.205
RP-24-S	−81.2	3.74	−47.3	0.190	MP-24-S	−78.6	3.69	−48.4	0.220
PPI-S	−73.7	3.69	−41.2	0.234					

agglomerates as well. Except for the affection of physical interaction between the PPI molecules and layered silicates, the breakage of PPI matrix might be augmented by the greater intercalated agglomerates of layered silicates, namely greater agglomerates of intercalated REC more severely destroyed the original microphase structure in PPI matrix and cleaved the entanglements among PPI molecules. As a result, the strengths of the RP-S nanocomposite sheets were even lower than PPI-S when the loading-level of REC was higher than 16 wt %. Meanwhile, all the MP-S nanocomposite sheets had higher strength than PPI-S.

CONCLUSION

In this work, the PPI was filled with MMT and REC by solution intercalation respectively, and then produced the reinforced PPI-based nanocomposites by hot press. In spite of the wider distance of interlayer in REC, the MMT with lower negative-charge surface and smaller apparent size of crude particles was easier to be exfoliated completely. However, the exfoliated REC nanoplatelets with more negative-charge could form stronger electrostatic interaction with positive-charge-rich domains of PPI molecules, and hence produced the highest strength in two series of nanocomposites. Although newly formed physical interactions between layered silicates and PPI molecules were weaker than the original state in PPI matrix, newly formed hydrogen bonds and electrostatic interaction on the surface of silicate lamellas provided the essential guarantee for the transfer of the stress to rigid layered silicates at least. In addition, the physical interaction between PPI molecules and layered silicates as well as the spatial occupancy of intercalated agglomerates destroyed the original microphase structure of PPI matrix and cleaved the entanglements among PPI molecules. It resulted in the decrease of elongation and strength, and especially for the high loading-level of layered silicates.

References

1. Mecking, S. Angew Chem Int Eng 2004, 43, 1078.
2. Sue, H. J.; Wang, S.; Jane, J. Polymer 1997, 38, 5035.
3. Kumar, R.; Choudhary, V.; Mishra, S.; Varma, I. K.; Mattiason, B. Ind Crop Prod 2002, 16, 155.
4. Zhang, J.; Jiang, L.; Zhu, L.; Jane, J. I.; Mungara, P. Biomacromolecules 2006, 7, 1551.
5. Darder, M.; Aranda, P.; Ruiz-Hitzky, E. Adv Mater 2007, 19, 1309.
6. Chen, P.; Zhang, L. Biomacromolecules 2006, 7, 1700.
7. Yu, L.; Dean, K.; Li, L. Prog Polym Sci 2006, 31, 576.
8. Ai, F.; Zheng, H.; Wei, M.; Huang, J. J Appl Polym Sci 2007, 105, 1597.
9. Zheng, H.; Ai, F.; Wei, M.; Huang, J.; Chang, P. R. Macromol Mater Eng 2007, 292, 780.
10. Wang, Y.; Cao, X.; Zhang, L. Macromol Biosci 2006, 6, 524.
11. Lu, Y.; Weng, L.; Zhang, L. Biomacromolecules 2004, 5, 1046.
12. Zheng, H.; Ai, F.; Chang, P. R.; Huang, J.; Dufresne, A. Polym Compos, 2009, 30, 474.
13. Wei, M.; Fan, L.; Huang, J.; Chen, Y. Macromol Mater Eng 2006, 291, 524.
14. Chen, P.; Zhang, L.; Peng, S.; Liao, B. J Appl Polym Sci 2006, 101, 334.
15. Usuki, A.; Hasegawa, N.; Kato, M. Adv Polym Sci 2005, 179, 135.
16. Yu, J.; Cui, G.; Wei, M.; Huang, J. J Appl Polym Sci 2007, 104, 3367.
17. Messersmith, P. B.; Giannelis, E. P. J Polym Sci Part A: Polym Chem 1995, 33, 1047.
18. Ma, X.; Liang, G.; Liu, H.; Fei, J.; Huang, Y. J Appl Polym Sci 2005, 97, 1915.
19. Zhu, J.; Morgan, A. B.; Lamelas, F. J.; Wilkie, C. A. Chem Mater 2001, 13, 3774.
20. Kojima, Y.; Usuki, A.; Kawasumi, M.; Okada, A.; Kurauchi, T.; Kamigaito, O. J Polym Sci Part A: Polym Chem 1993, 31, 983.
21. Usuki, A.; Kawasumi, M.; Kojima, Y.; Okada, A.; Kurauchi, T.; Kamigaito, O. J Mater Res 1993, 8, 1174.
22. Huang, J.; Zhu, Z.; Yin, J.; Qian, X.; Sun, Y. Polymer 2001, 42, 873.
23. Yao, Q.; Wang, C.; Zhao, L. Miner Res Geol 2001, 15, 264.
24. Grim, R. E.Clay Mineralogy; McGraw-Hill: New York, 1968.
25. Ray, S. S.; Okamoto, M. Prog Polym Sci 2003, 28, 1539.
26. Johnston, C. T.; Premachandra, G. S. Langmuir 2001, 17, 3712.
27. Ras, R. H. A.; Johnston, C. T.; Franses, E. I.; Ramaekers, R.; Maes, G.; Foubert, P.; De Schryver, F. C.; Schoonheytdt, R. A. Langmuir 2003, 19, 4295.
28. Sohn, J. R.; Kim, J. T. Langmuir 2000, 16, 5430.
29. Consultchi, A.; Cordova, I.; Valenzuela, M. A.; Acosta, D. R.; Bosch, P.; Lara, V. H. Energy Fuels 2005, 19, 1417.
30. Adachi, M.; Kanamori, J.; Masuda, T.; Yagasaki, K.; Kitamura, K.; Mikami, B.; Utsumi, S. Proc Natl Acad Sci USA 2003, 100, 7395.
31. Ray, S. S.; Okamoto, K.; Okamoto, M. Macromolecules 2003, 36, 2355.
32. Hudson, S.; Magner, E.; Cooney, J.; Hodnett, B. K. J Phys Chem B 2005, 109, 19496.
33. Ruso, J. M.; Doe, N.; Somasundaran, P. Langmuir 2004, 20, 8988.